CHEMICAL ENGINEERING TRANSACTIONS
VOL. 94, 2022
A publication of AIDIC
The Italian Association of Chemical Engineering
Online at www.cetjournal.it
Guest Editors: Petar S. Varbanov, Yee Van Fan, Jiří J. Klemeš, Sandro Nižetić

ISBN 978-88-95608-93-8; **ISSN** 2283-9216
DOI: 10.3303/CET2294060

Selective Adsorptive Recovery of Platinum from Spent Catalytic Converter

Lawrence A. Limjuco*, Joey D. Ocon

Laboratory of Electrochemical Engineering (LEE), Department of Chemical Engineering, University of the Philippines Diliman, Quezon City, Philippines, 1101
lalimjuco@up.edu.ph

Ethylene glycol dimethacrylate (EGDMA) – dithiadiamide (DTDA) copolymer was synthesized by condensation reaction between monomeric mercaptoacetamide and ω-dibromoalkanes. This previously designed DTDA was complexed with Pt^{2+} before direct copolymerization with EGDMA. Pt^{2+}-template was eluted with dilute HCl. The EGDMA-DTDA copolymer was evaluated for Pt^{2+} adsorption in terms of adsorption isotherm and selectivity. The copolymer exhibited monolayer Langmuir-type adsorption isotherm with q_m = 177 mg g^{-1} at optimum pH = 1. It is selective to Pt^{2+} in a simulated solution containing the predominant cations present in an acid-leached spent 3-way, gasoline automobile catalytic converter sample (i.e., Al^{3+}, Ba^{2+}, Ce^{3+}, Fe^{2+}, Mg^{2+}, and Zn^{2+}).

1. Introduction

Platinum, being a critical raw material (European Commission, 2019), can be considered as integral element for sustainable technologies for fight against climate change. Platinum (Pt) and palladium (Pd) oxidizes harmful CO and hydrocarbon to CO_2 and H_2O, they find use in automobile catalytic converters (ACC) (Sun et al., 2022). Pt is also employed as catalyst in both anode and cathode for proton exchange membrane fuel cells (Granados-Fernández et al., 2021). Pt, due to its resistance to corrosion, chemical inertness, thermal stability, and catalytic property, has been crucial for different chemical and electrochemical processes and hence, finds increasing demand (Granados-Fernández et al., 2021). Its criticality, compounded by their low substitutability and restricted reserve distributions, (European Commission, 2019) calls for recovery from secondary sources.

Pt concentration in ACC can be significant (~2,000 g t^{-1}) in comparison to natural ores (~10 g t^{-1}) (Sun et al., 2022). Other parameters such as energy cost (1,400 – 3,400 MJ vs. 18,860 – 254,860 MJ/kg of metal) and natural resources used (3,000 – 6,000 m^3 vs. 100,000 – 1,200,000 m^3 of water per t of metal extracted) make recycling from end-of-life products like ACC highly viable and advantageous than extracting it from primary sources such as natural ores (European Commission, 2019).

Although the abundant Pt-complexing functional groups of many sustainable and cheap biomass-based sorbents render the material with high adsorption capacity (q_e), it may limit the Pt selectivity (Wang et al., 2017). Meanwhile, molecular recognition technology has been recently explored to have industrial application for Pt separation from process streams (Izatt et al., 2011). While molecular ion imprinting technology has been explored for the selective sequestration of cationic analytes (Izatt et al., 2011), it has not been much explored for Pt recovery from secondary sources.

Previously designed dithiadiamide (DTDA) ligand (Gxoyiya 2003) has been synthesized and evaluated for Pt recovery from acid-digested spent ACC. The DTDA ligand has been copolymerized with minimal amount of ethylene glycol dimethacrylate (EGDMA) to optimize the copolymer's q_e. The morphology of the copolymer was normalized with that of the control (i.e., poly-EGDMA) and characterized to eliminate the possible morphological factor on the performance of the EGDMA-DTDA copolymer vs. that of the poly-EGDMA. Adsorption isotherm was evaluated to determine the q_m. Finally, the selectivity of the copolymer was evaluated using simulated feed solution containing the predominant cations present in actual acid-digested spent ACC.

Paper Received: 15 April 2022; Revised: 07 June 2022; Accepted: 12 June 2022
Please cite this article as: Limjuco L.A., Ocon J.D., 2022, Selective Adsorptive Recovery of Platinum from Spent Catalytic Converter, Chemical Engineering Transactions, 94, 361-366 DOI:10.3303/CET2294060

2. Methodology

Synthesis of ethylene glycol dimethacrylate (EGDMA) – dithiadiamide (DTDA) copolymer was synthesized using modified procedure from the literature (Gxoyiya, 2003).

2.1 Dithiadiamide ligand

KOH solution (2.36 g in 2 mL H_2O) was added to 4-acetamidophenol solution (34 mmol in 25 mL EtOH). Allyl bromide (37 mmol) was then added dropwise. The reaction solution was boiled under reflux and terminated with deionized (DI) water. Precipitated solid was filtered and recrystallized from dilute EtOH to yield *N*-(4-(allyloxy)phenyl)acetamide 1. Intermediate 1 (27 mmol) was then acid hydrolyzed in 20 % H_2SO_4 at elevated temperature under reflux. Gradual cooling at 5 ^oC precipitated fine crystals which were re-dissolved in hot DI water with pH adjusted to 11 using NaOH solution. Resulting amine was extracted using diethyl ether which was subsequently evaporated *in vacuo* to yield 4-(allyloxy)aniline 2 (5.5 mmol). This was subsequently reacted with 2-mercaptoacetic acid (5.5. mmol) under N_2 atmosphere for 3 h at 90 ^oC. Precipitated solid upon cooling at room temperature was crushed into fine powder under DI water. This was then filtered and washed sequentially with dilute HCl and DI water and recrystallized from aqueous EtOH to yield *N*-(4-allyloxyphenyl)-2-mercaptoacetamide 3 (1.4 mmol). This was dissolved in equimolar KOH (1.4 mmol) solution in MeOH (60 mL). *ω*-dibromoalkane (0.7 mmol) in MeOH (10 mL) was then added dropwise. The reaction was carried out at room temperature for 24 h before quenching it with DI water. The MeOH was evaporated *in vacuo* while the residual aqueous phase was extracted with EtOAc. The combined extracts were dried with anhydrous $MgSO_4$. The dithiadiamide (DTDA) was purified via recrystallization from EtOH.

2.2 EGDMA-DTDA copolymer

DTDA ligand (0.1 mmol) in MeOH (25 mL) was added dropwise to K_2PtCl_4 (0.1 mmol) solution in MeOH (10 mL). The mixture was stirred for 48 h to yield white precipitate which was then washed with MeOH and dried *in vacuo* to yield the Pt-DTDA ligand complex. This complex was dissolved in DMF (3 mL). EGDMA was added under N_2. Catalytic amount of AIBN (0.1 mmol) was added and the mixture was heated at 65 ^oC for 4-12 h. The resulting yellow solid was washed sequentially with $CHCl_3$ and MeOH, dried in vacuo, then washed with 0.5 M HCl and DI water to remove the Pt-template to produce the Pt-templated EGDMA-DTDA copolymer. Known amount of the copolymer (50 mg) was soaked in 10 mL 0.5 M HCl and vigorously vortexed. The solids were vacuum filtered and rinsed with DI water.

2.3 Analyses and characterization

Starting precursors, intermediates, and products were analyzed using attenuated total reflectance (ATR) - Fourier transform infrared (FTIR) spectroscopy (Agilent Technologies, USA) to monitor the synthesis reaction. Structures of the intermediates and products were confirmed via ^{13}C NMR (400 MHz Varian, USA) using deuterated chloroform ($CDCl_3$) or dimethyl sulfoxide (DMSO-d_6) as solvents.

Nitrogen adsorption/desorption isotherms were determined using Belsorp-mini II (Bel Japan, Inc) at relative pressure range ($p\ p_o^{-1}$) between 0.01 and 1.0. Brunauer–Emmett–Teller (BET) surface area was determined from the BET plot while pore size distributions were calculated using Barrett–Joyner–Halenda (BJH) method.

Concentrations of the different metal ions were quantified using inductively coupled plasma mass spectrometry (ICP-MS, Agilent 7500 series). Liquid samples such as feed, ligand copolymer-treated solutions, and HCl washings were collected and passed through 0.2 µm Nylon syringe filters. Sample aliquots were acid digested (5 mL sample + 10 mL DI + 3 mL 60% RHM HNO_3) via microwave irradiation (MARS-5 CEM) and diluted to 100-mL polypropylene volumetric flasks prior ICP-MS analysis.

3. Results and Discussion

Synthesis of the MIIP involves three major phases (Figure 1a): a) formation of monomeric mercaptoacetamide **3**; b) condensation of two monomeric **3** with *ω*- dibromoalkanes to yield the DTDA ligand followed by complexation with Pt^{2+}; and c) polymerization of Pt-ligand complex with EGDMA and subsequent elution of Pt^{2+} to yield the Pt-templated EGDMA-DTDA copolymer. Starting material, intermediates, and final ligands were confirmed via FTIR (Figure 1b) and ^{13}C NMR (Figure 2).

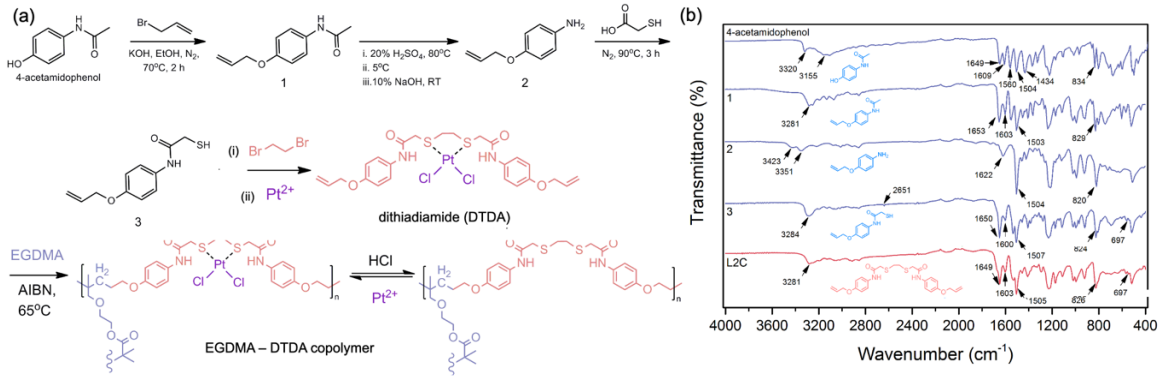

Figure 1: Synthesis of EGDMA-DTDA copolymer: (a) synthesis route and (b) FTIR of starting material, intermediates, and final product.

Starting material 4-acetamidophenol contains three fundamental functional groups: (1) secondary amide is depicted by single peak at 3,320 cm^{-1}. Strong peak at 1,649 cm^{-1} can be attributed to the C=O while the peak at 1,560 cm^{-1} is due to the combined C-N and N-H stretching; (2) the -OH group can be observed from the broad peak at 3,155 cm^{-1} (Pavia et al., 2001); (3) the aromatic ring can be confirmed from the C=C stretching between 1,600 cm^{-1} and 1,450 cm^{-1} peaks while the *para*-di-substitution is exhibited by the strong band between 850 – 800 cm^{-1} (Pavia et al., 2001) which are present in all intermediates and products. 4-acetamidophenol was reacted with allyl bromide in methanolic KOH to yield *N*-(4-(allyloxy)phenyl)acetamide 1 at high yield (85 %). Disappearance of the -OH band of 4-acetamidophenol suggests the successful allylation while peak at 3,281 cm^{-1} can be attributed to the N-H stretching. More intense peak at 1,653 cm^{-1} can be assigned to the overlapping C = O (1,680 – 1,630 cm^{-1}) of the amide and C = C (1,660 – 1,600 cm^{-1}) of the vinyl groups (Pavia et al., 2001). Subsequent acid hydrolysis of 1 yielded 4-(allyloxy)aniline 2 at acceptable yield (63 %). The appearance of two bands at 3,423 and 3,351 cm^{-1} confirms the conversion of secondary amide of 1 to primary amine of 2 (Pavia et al., 2001). This can also be confirmed from the disappearance of C = O stretching of the amide in the region 1,630 – 1,680 cm^{-1}. Less intense peak at 1,622 cm^{-1} can be associated to the C=C of the vinyl group (Gxoyiya et al., 2003).

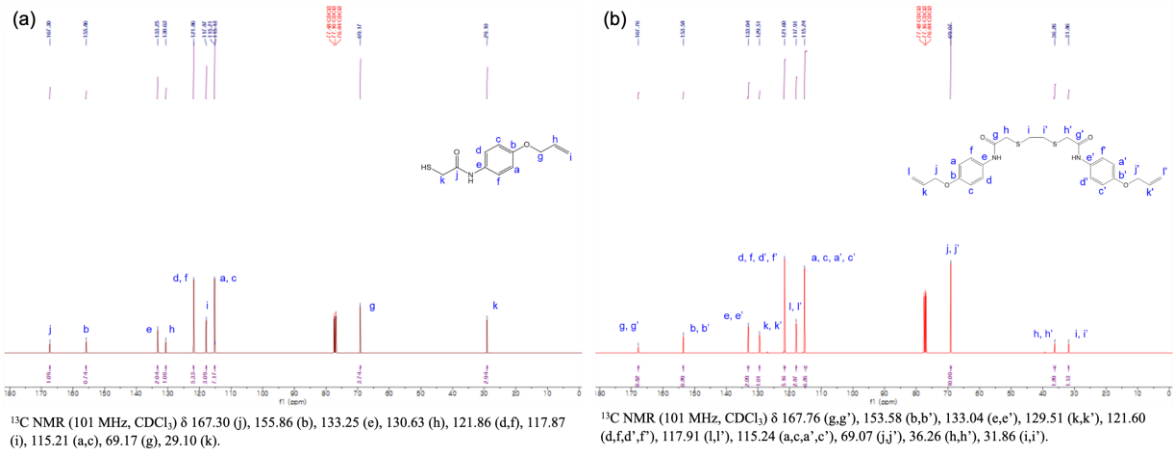

Figure 2: ^{13}C NMR of a) N-(4-(allyloxy)phenyl)-2-mercaptoacetamide denoted as intermediate 3 (yield = 52 %) and b) of 2,2'-(ethane-1,2-diylbis(sulfanediyl))bis(N-(4-(allyloxy)phenyl) acetamide) denoted as DTDA (yield = 64 %).

The mercaptoacetamide **3** was prepared by condensation reaction between **2** and mercaptoacetic acid and was purified by recrystallization from EtOH-H_2O mixtures. Product was isolated in moderate yield (52 %) and was also confirmed by spectroscopic analysis. The disappearance of the two primary amine peaks of **2** and the appearance of single peak at 3,284 cm^{-1} can be regarded as the conversion of the amine to the amide of **3**. This is supported by the emergence of peak at 1,650 cm^{-1} which can be associated to the C = O of the amide (Pavia et al., 2001). Peak at 1,600 cm^{-1}, which is present up to the final products, can be attributed to the C = C of the

vinyl group. Lastly, weak peaks at 2,651 and 697 cm^{-1} can be attributed to the S - H and C - S stretching, of the thiol group of **3** (Rao et al., 1964).

Monomeric **3** was coupled with *ω*-dibromoalkanes at 2:1 mole ratio in methanolic KOH. Purification was conducted by recrystallization from EtOH and the diamide products were isolated in reasonable yields (64 - 71 %). FTIR showed similar spectra of the ligand which resemble that of **3** (Figure 1b). While very weak S - H peak at 2,651 cm^{-1} was detected in **3**, this was not observed among ligands though C-S stretching at 570 -710 cm^{-1} were present. Similarly, the ^{13}C NMR of the DTDA (Figure 2b) resemble that of **3** (Figure 2a) except the appearance of extra signal in the methylene regions δ 30 - 40 ppm. This confirms the successful coupling of the monomer **3** with *ω*-dibromoalkanes to yield the bidentate DTDA ligand (Gxoyiya 2003).

White poly-EGDMA and yellowish-brown EGDMA-DTDA copolymer show different optical images (Figure 3a inset). To eliminate the factor of morphological differences on the performance of the poly-EGDMA and EGDMA-DTDA copolymer, N_2 adsorption-desorption isotherms at 77 K (Figure 3a) and pore size distribution analysis via BJH model (Figure 3b) were conducted. Both exhibited type IV isotherm indicating that samples are mesoporous and that adsorption proceeds in multilayer followed by capillary condensation (Gong et al., 2016). Type H1 hysteresis suggests that all samples have high degree of pore size uniformity which was confirmed from the narrow pore size distribution obtained using BJH model (Figure 3b) with mean pore diameter = 4.62 nm (poly-EGDMA) and 4.66 nm (EGDMA-DTDA). Both samples have comparable pore volume (0.16 $cm^3\ g^{-1}$) and surface area (162.71 $m^2\ g^{-1}$ for poly-EGDMA and 158.06 $m^2\ g^{-1}$for EGDMA-DTDA) obtained from the BET plot (Figure 3b inset). These morphological similarities of the poly(EGDMA) and EGDMA-DTDA copolymer can suggest that differences in the adsorption performance of the materials cannot be attributed to the normalized morphologies and can be mainly due to the molecular component of the adsorbents.

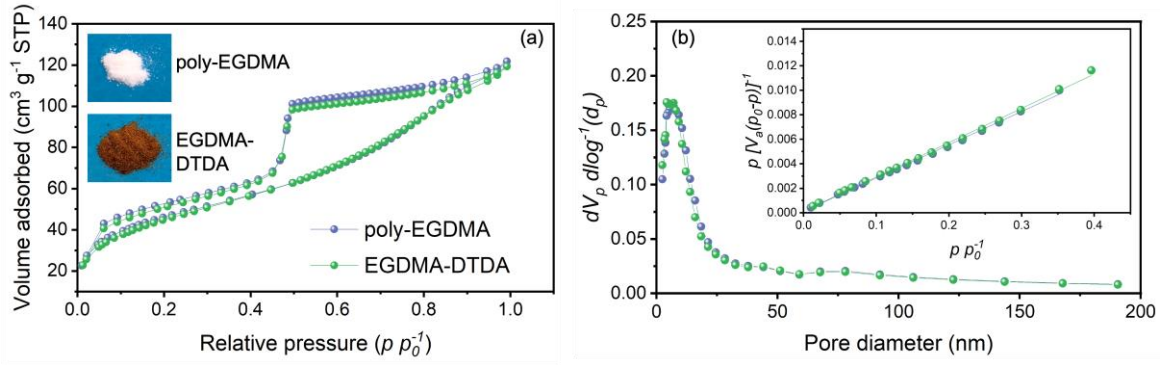

Figure 3: Morphological characterizations of the MIIPs: (a) N2 adsorption–desorption curves (inset: optical images); and (b) pore size distribution via BJH model (inset: BET plots).

Effect of pH on the adsorption capacity of the EGDMA-DTDA copolymer was first evaluated since pH, together with Cl^- and Pt^{2+} concentrations, affects the speciation of the Pt^{2+}. Adsorption capacity (q_e) of the EGDMA-DTDA copolymer decreases with increasing pH (Figure 4a). At low, HCl-controlled pH (e.g., 0.1 M HCl), Cl^- concentration is high enough to promote the formation of chloro-anionic species (e.g., $PtCl_4^{2-}$ and $PtCl_3^-$) (Figure 4b). These can be readily adsorbed by donor atoms of the copolymer (e.g., N and/or S) (Chassary et al., 2005). At lower Cl^- concentration (e.g., 0.01 M HCl for pH = 2) (Figure 4c), Pt^{2+} species are less adsorbable (Chassary et al., 2005) and pH = 1 was chosen for the batch adsorption experiments.

Adsorption isotherm experiments were conducted at different Pt^{2+} initial concentrations (C_o = 10 - 200 mg L^{-1}). The q_e's were fitted on non-linear Langmuir (Eq. 1) and Freundlich (Eq. 2) isotherm models:

$$q_e = \frac{q_m K_L C_e}{1 + K_L C_e} \tag{1}$$

$$q_e = K_F C_e^{\frac{1}{n}} \tag{2}$$

where q_m and K_L are the maximum adsorption capacity and Langmuir constant, respectively while K_F is the Freundlich constant for the adsorption capacity while n is for the adsorption intensity (Rostamian et al., 2011).

The control poly-EGDMA follows Langmuir-type adsorption isotherm and has minimal q_m = 12.15 mg g^{-1} (Table 1) indicating that the adsorption capacity of the EGDMA-DTDA copolymer can be mainly due to the DTDA component.

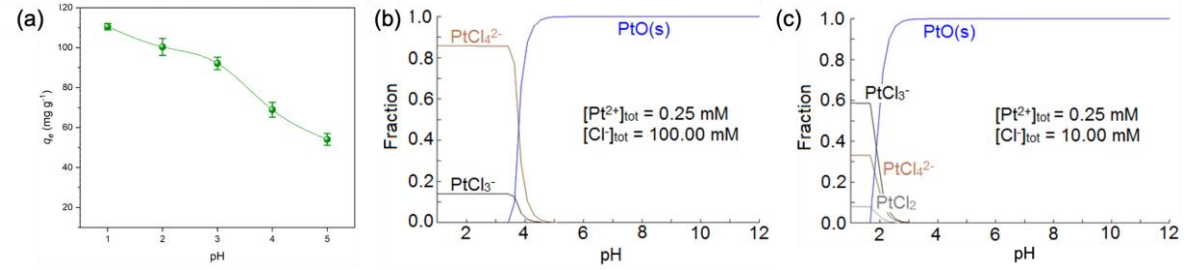

Figure 4: Adsorption performance evaluation. Effect of pH: (a) q_e of MIIPs at different pH [C_o = 50 mg Pt^{2+} L^{-1}; V = 30 mL; m = 10 mg; T = 30ºC; 300 rpm; t = 12 h]; speciation of Pt^{2+}using Hydra-Medusa® equilibrium diagram software (C_o ≈ 50 mg L^{-1}) at (b) 0.1 M HCl and (c) 0.01 M HCl.

Pt^{2+} adsorption on EGDMA-DTDA copolymer can be characterized by the monolayer Langmuir-type than the Freundlich model as suggested by better correlation, R^2 > 0.99 with maximum Pt^{2+} capacity, q_m = 177.22 mg g^{-1}(Table 1). While this q_m are lower than chitosan-based biosorbents such as glycine-modified persimmon powder (250 mg g^{-1}) (Gong et al., 2016), this is better than polythyleneimine-modified biomass (122 – 154 mg g^{-1}) (Garole et al., 2018) and organic adsorbents synthesized such as dibenzo-18-crown-6 grafted polymer (84 mg g^{-1}) (Talanova et al., 2000).

Table 1: Adsorption performance of poly-EGDMA and EGDMA-DTDA copolymer [V = 30 mL; m = 10 mg; pH = 1; T = 30 ºC; 300 rpm; t = 12 h].

Samples	Freundlich			Langmuir		
	n	K_f (mg g^{-1})	R^2	K_L (x 10^{-3} L mg^{-1})	q_m (mg g^{-1})	R^2
Poly-EGDMA	1.47	0.49	0.96	1.65	12.15	> 0.99
EGDMA-DTDA	1.86	15.54	0.90	10.89	177.22	> 0.99

The EGDMA-DTDA copolymer was tested on a simulated solution of predominant cations present in acid-digested automobile catalytic converter (ACC) to evaluate its selectivity. ICP-MS semi-quantitative analysis of actual spent ACC (data not shown) reveals that the most abundant elements present in the sample are Al^{3+}, Ba^{2+}, Ce^{3+}, Fe^{2+}, Mg^{2+}, and Zn^{2+} which constitute the support cordierite ($2MgO•2Al_2O_3•5SiO_2$), additives in the washcoat (e.g., Ce and Fe) and alkaline-earth (e.g., Ba) (Garole et a., 2018). These elements were selected as competing cations for Pt^{2+} in the selectivity study.

Table 2: Selectivity of EGDMA-DTDA copolymer to Pt^{2+} from other major cations in acid-leached spent ACC [$C_{o\ M}{}^{n+}$ ≈ 20 mg L^{-1}; V = 30 mL; m = 10 mg; pH = 1; T = 30 ºC; 300 rpm; t = 12 h].

Cations	C_o (mg/L)	C_o (mmol L^{-1})	C_e (mmol L^{-1})	q_e (mmol g^{-1})	K_d (mL/g)	α ($K_{d\ Pt/M}$)	CF x 10^{-3} (L/g)
Pt^{2+}	**19.17 ± 0.53**	**0.10**	**0.00**	**0.30**	**99,858.2**	**1.0**	**3,093.0**
Mg^{2+}	19.48 ± 0.46	0.80	0.76	0.12	155.5	642.2	148.3
Al^{3+}	14.94 ± 0.42	0.55	0.54	0.05	94.5	1057.5	91.8
Fe^{2+}	19.60 ± 0.16	0.35	0.33	0.07	197.2	506.6	185.7
Zn^{2+}	20.98 ± 0.02	0.32	0.32	0.01	47.1	2122.0	46.4
Ba^{2+}	19.81 ± 1.02	0.14	0.14	0.02	149.3	669.9	142.6
Ce^{3+}	20.92 ± 0.14	0.15	0.14	0.03	189.7	529.5	178.9

Results (Table 2) show that EGDMA-DTDA copolymer is selective to Pt^{2+} where q_e follows the following order: Pt^{2+} > Mg^{2+} > Fe^{2+} > Al^{3+} > Ce^{3+} > Ba^{2+} > Zn^{2+}. No conclusive trend in terms of the hard-soft properties of the cations can be derived from the experimental result given that Zn^{2+} and Fe^{2+} are borderline soft-hard acid while Mg^{2+}, Ba^{2+}, Ce^{3+}, and Al^{3+} are hard acids as compared to the soft Pt^{2+}. The measured q_e values of other cations can be attributed to non-selective adhesion to other components of the MIIP (i.e., EGDMA). Nonetheless, selectivity to Pt^{2+} was further reflected by the significantly higher K_d (99,858). The obtained α value indicate high

separation efficiency of Pt^{2+} from other cations and that it has been concentrated *CF* = 3,100 times while other cations were enriched at significantly lower degrees. This features advantage of EGDMA-DTDA copolymer as compared to biosorbents which have very limited to no selectivity to Pt^{2+} as presented by their $\alpha_{\frac{Pt}{M}} < 1$, indicating it is more selective to other metals such as Au and Pd or limited $\alpha_{\frac{Pt}{M}} \leq 50$ with respect to other base metals such as Zn and Cu (Wang et al., 2017).

4. Conclusions

Effectivity of the previously designed dithiadiamide (DTDA) ligand copolymerized with ethylene glycol dimethacrylate (EGDMA) on the adsorptive recovery of Pt^{2+} from spent automobile catalytic converter was demonstrated. Minimal amount of EGDMA was copolymerized to maximize the potential performance of the DTDA. Both control poly-EGDMA and EGDMA-DTDA copolymer follow Langmuir type adsorption isotherm with calculated q_m = 177.22 and 12.15 mg g^{-1}. The EGDMA-DTDA copolymer exhibited superior selectivity towards Pt^{2+} as compared to other predominant cations present in actual digested 3-way type spent ACC which could be mainly due to the imprinting of Pt^{2+} to the DTDA prior EGDMA copolymerization. This study supports the potential of molecular recognition technique as effective approach for selective recovery of critical raw materials like platinum.

Acknowledgments

The authors would like to acknowledge the DOST-NICER R&D Center for Advanced Batteries Program funded by the Department of Science and Technology (DOST) and the CIPHER Project (IIID-2018-008) funded by The Commission on Higher Education through the Philippine California Advanced Research Institutes Program. L.A. Limjuco would like to acknowledge the Balik Scientist Program of the DOST for his award as a returning scientist.

References

Chassary P., Vincent T., Sanchez Marcano J., Macaskie L.E., Guibal E., 2005, Palladium and platinum recovery from bicomponent mixtures using chitosan derivatives, Hydrometallurgy, 76, 131–147 .

European Commission, 2019, Critical Raw Materials; European Commission Report; European Commission: Brussels, Belgium.

Garole D.J., Choudhary B.C., Paul D., Borse A.U., 2018, Sorption and recovery of platinum from simulated spent catalyst solution and refinery wastewater using chemically modified biomass as a novel sorbent, Environmental Science and Pollution Research, 25, 10911–10925.

Gong Q.Q., Guo X.Y., Liang S., Wang C., Tian Q.H., 2016, Study on the Adsorption Behavior of Modified Persimmon Powder Biosorbent on Pt(IV), International Journal of Environmental Science and Technology, 13, 47–54.

Granados-Fernández R., Montiel M.A., Díaz-Abad S., Rodrigo M.A., Lobato J., 2021, Platinum Recovery Techniques for a Circular Economy, Catalysts, 11, 937–952.

Gxoyiya B.S.B., 2003, Synthesis and evaluation of PGM-selective ligands, MSc Dissertation, Rhodes University, Grahamstown, South Africa.

Izatt R.M., Izatt S.R., Izatt N.E., Krakowiak K.E., Bruening R.L., Navarro L., 2015, Industrial applications of Molecular Recognition Technology to separations of platinum group metals and selective removal of metal impurities from process streams, Green Chemistry, 17, 2236–2245.

Pavia D.L., Lampman G.M., Kriz G.S. (Third Ed), 2001, Introduction to Spectroscopy, A Guide for Students of Organic Chemistry, Brooks/Cole, Massachusetts, USA.

Rao C.N.R., Venkataraghavan R., Kasturi T.R., 1964, Contribution to the infrared spectra of organosulphur compounds, Canadian Journal of Chemistry, 42, 36-42.

Rostamian R., Najafi M., Rafati A.A., 2011, Synthesis and Characterization of Thiol-Functionalized Silica Nano Hollow Sphere as a Novel Adsorbent for Removal of Poisonous Heavy Metal Ions from Water: Kinetics, Isotherms and Error Analysis, Chemical Engineering Journal, 171, 1004–1011.

Sun S., Jin C., He W., Li G., Zhu H., Huang J., 2022, A review on management of waste three-way catalysts and strategies for recovery of platinum group metals from them, Journal of Environmental Management, 305, 114383–114394.

Talanova G.G., Yatsimirskii K.B., Kravchenko O.V., 2000, Peculiarities of K_2PdCl_4 and K_2PtCl_4 Complexation with Polymer-Supported Dibenzo-18-crown-6, Industrial & Engineering Chemistry Research, 39, 3611–3615.

Wang S.Y., Vincent T., Roux J.C., Faur C., Guibal E., 2017, Pd(II) and Pt(IV) sorption using alginate and algal-based beads, Chemical Engineering Journal, 313, 567–579.